

# REGRAD: A Large-Scale Relational Grasp Dataset for Safe and Object-Specific Robotic Grasping in Clutter

Hanbo Zhang\*, Deyu Yang\*, Han Wang\*, Binglei Zhao, Xuguang Lan ✉, Jishi Yu Ding, Nanning Zheng

**Abstract**—Despite the impressive progress achieved in robotic grasping, robots are not skilled in sophisticated tasks (e.g. search and grasp a specified target in clutter). Such tasks involve not only grasping but the comprehensive perception of the world (e.g. the object relationships). Recently, encouraging results demonstrate that it is possible to understand high-level concepts by learning. However, such algorithms are usually data-intensive, and the lack of data severely limits their performance. In this paper, we present a new dataset named REGRAD for the learning of relationships among objects and grasps. We collect the annotations of object poses, segmentations, grasps, and relationships for the target-driven relational grasping tasks. Our dataset is collected in both forms of 2D images and 3D point clouds. Moreover, since all the data are generated automatically, it is free to import new objects for data generation. We also released a real-world validation dataset to evaluate the sim-to-real performance of models trained on REGRAD. Finally, we conducted a series of experiments, showing that the models trained on REGRAD could generalize well to the realistic scenarios, in terms of both relationship and grasp detection. Our dataset and code could be found at: <https://github.com/poisonwine/REGRAD>.

## I. INTRODUCTION

Robotic grasping is a fundamental problem in robotics. It plays a basic role in nearly all robotic manipulation tasks. Particularly, visual perception is important for robotic grasping, since it can provide rich observations about the surroundings. Recently, with deep learning, robotic grasping has achieved impressive progress. For example, the deep-learning methods [1]–[3] achieved state-of-the-art performance on different benchmarks with surprisingly good generalization to unknown objects. However, grasping in realistic scenarios is usually target-driven, which often requires the understanding of high-level visual concepts, e.g., the object relationships. Though currently, to some extent, we can generate stable grasps in either scattered or cluttered scenes based on the advanced grasping algorithms, it is still hard for the robot to complete sophisticated manipulation tasks.

Suppose a common scene in our life as shown in Figure 1. If we want the robot to get the bottom plate for us, how can the robot achieve it? Such a sophisticated task is obviously

\* Equally contributed.

Corresponding Author: Xuguang Lan. Xuguang Lan is with the Institute of Artificial Intelligence and Robotics, the National Engineering Laboratory for Visual Information Processing and Applications, School of Electronic and Information Engineering, Xi’an Jiaotong University, No.28 Xianning Road, Xi’an, Shaanxi, China. [xgлан@mail.xjtu.edu.cn](mailto:xgлан@mail.xjtu.edu.cn)

This work was supported in part by the key project of Trico-Robot plan of NSFC under grant No. 91748208, National Key Program of China No.2017YFB1302200, key project of Shaanxi province No.2018ZDCXL-GY-06-07, and NSFC No.61573268.

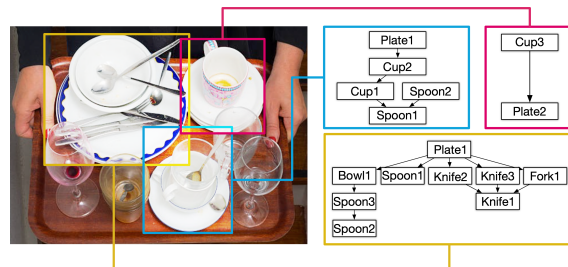


Fig. 1: An example of a sophisticated target-driven grasping task in dense clutter. **Left**: the working scenario. **Right**: the correct grasping order among objects. Obviously, grasping without understanding the high-level visual concepts (e.g. relationships among objects and grasps) will result in a failure and even severe damages to other objects.

much harder than just finding a stable grasp of some object and raises two main challenges:

- **The understanding of object relationships** is necessary for inferring the correct grasping order shown on the right of Figure 1. Otherwise, it may cause irrevocable damages to other objects.
- The robot is required to perform **object-specific grasping** in dense clutter, which causes severe overlaps and occlusions among objects.

Previous works [4], [5] explored the manipulation relationship detection and object-specific grasping in clutter. However, such deep learning methods are usually data-intensive [6]. The dataset, VMRD [4], containing only 200 object instances restricted their generality in real-world scenarios, and the human bias in VMRD exacerbates the overfitting since the model inevitably encoded the bias during learning. To solve these problems, in this paper, we propose a novel, large-scale, and automatically-generated dataset. By considering the relationships among objects and grasps, our dataset, called RElational GRAsp Dataset (REGRAD), aims to build a benchmark for relational grasping in dense clutter. Our dataset has the following features:

- **More objects and categories.** Our dataset is built upon the well-known ShapeNet dataset [10], [11], including 55 categories and 50K different object models.
- **Different kinds of modalities** including the depth images and point clouds, which are helpful for relationship detection, grasp synthesis, and sim-to-real transferring.
- **Rich labels** including:
  - 6D pose of each object.
  - Bounding boxes and segmentations on 2D images.

TABLE I: Comparison with Related Datasets

Dataset	Num Imgs	Modality	Obj. /Img	Grasps /Img	Grasp Label	Type	Rel. Label	6D Pose	Seg. Label	Num Cat.	Num Obj.	Num Rel.	Num Grasps
Cornell	1035	RGB-D	1	~8	Rect	Real	-	×	×	-	240	0	8K
Mahler et al. [2]	6.7M	Depth	1	1	Rect	Sim	-	×	×	-	1500	0	6.7M
Levine et al. [7]	800K	RGB-D	-	1	Rect	Real	×	×	×	-	-	0	800K
Jacquard [8]	54K	RGB-D	1	~20	Rect	Sim	-	×	✓	-	11K	0	1.1M
VMRD [4]	4.7K	RGB	~3	~20	Rect	Real	✓	×	×	31	~200	46K	100K
GraspNet [9]	97K	RGB-D	~10	3~9M	Rect+ 6D	Real	×	✓	✓	-	88	0	1.2B
<b>REGRAD</b>	<b>900K</b>	RGB-D	1~20	1.02K	Rect+ 6D	Sim	✓	✓	✓	55	50K	12M	100M

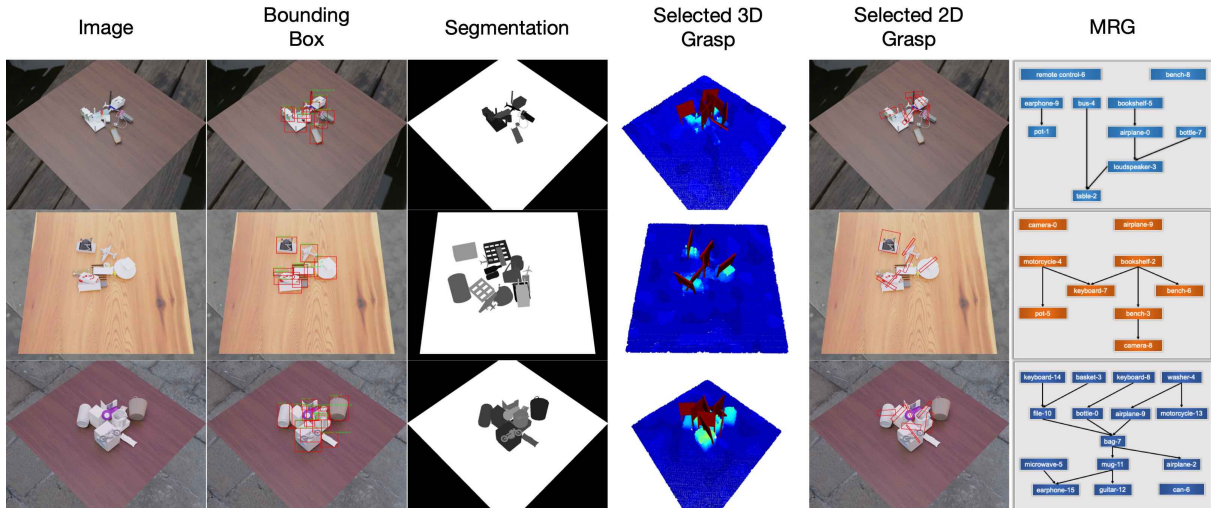


Fig. 2: Some examples of REGRAD. The images are taken from 9 different views and the background is randomly generated. From left to right: **Image**: the original RGB image of the scene; **Bounding Box**: the minimal vertical rectangle to cover all pixels of the object; **Segmentation**: the pixel-wise segmentation, with different pixel values representing different objects; **Selected 3D Grasp**: the visualization of a selected subset of 6D grasp labels in the 3D working space; **Selected 2D Grasp**: the rectangular (Rect.) grasp representation in the 2D image space, with center  $(x, y)$ , width  $w$ , height  $h$ , and the orientation  $\theta$ ; **MRG**: manipulation relationship graph representing the correct order of grasping.

- Point cloud segmentations.
- Manipulation Relationship Graph (MRG) indicating the grasping order.
- Collision-free and stable 6D grasps of each object.
- Rectangular 2D grasps.
- **Segregated training, validation, and test sets** including the unseen validation set and unseen test set, in which the objects belong to unknown categories.
- **Multi-view data** which releases the assumption of single-view perception since in practice the robot could move around for more precise manipulation.
- **Automatic data generation** in the physical simulator which will save much time to label the dataset and avoid the bias from the human labels. Currently, to add new objects to the datasets, we only need to scan the 3D models instead of re-collecting and labeling images. We also provide the open-source codes for dataset generation<sup>1</sup>.

Currently, our dataset contains 111.8k different scenes, including 46.9k training scenes, 32.1k validation scenes,

and 32.8k test scenes. To validate the trained models with unknown objects, the validation set and the test set are split into two parts: the *seen* and *unseen* parts. Figure 2 shows some examples of our dataset. The quantitative comparison with other existing datasets could be found in Table I.

In summary, our contributions include:

- We propose to automatically label the manipulation relationships by leveraging the physical simulators, avoiding the expensive manual labeling as well as the human bias, which exacerbates the overfitting.
- We contribute a large-scale relational grasping dataset named REGRAD. As we know, it is the first large-scale relational grasping dataset.
- We validate the sim-to-real performance of both manipulation relationship detection and grasp detection on REGRAD, and the results show that the models trained on REGRAD could surprisingly transfer to realistic scenarios only by proper domain randomization techniques.

<sup>1</sup><https://github.com/poisonwine/REGRAD>

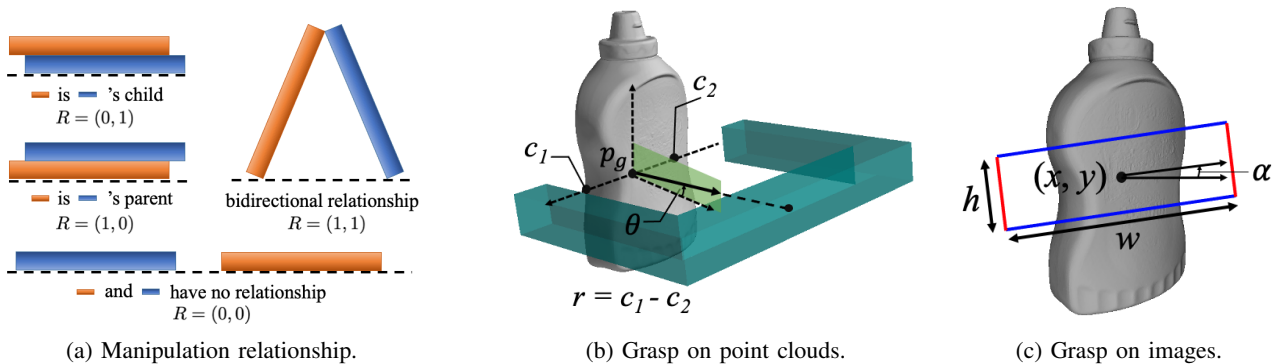


Fig. 3: Modeling of manipulation relationships and grasps in our dataset.

## II. RELATED WORK

**Visual Relationship** [12] is related to our manipulation relationship. It is defined as the relationship between objects inferred from visual images. Recently, a number of datasets have appeared, including the Visual Relationship Dataset [12] and Visual Genome [13]. Inspired by these works, Visual Manipulation Relationship Dataset (VMRD) [4] is proposed for robotic manipulation relationship detection. Yet there are several drawbacks making models trained on VMRD not generalize well to realistic scenes: 1) VMRD only contains RGB images; 2) VMRD contains human biases when collected; 3) The data is limited due to expensive manual labeling.

**Spatial relation and support relation** are also related to the manipulation relationship. There are several works focusing on spatial relations in clutter (e.g. [14]). However, spatial relations cannot be directly used to guide the manipulation in clutter. Another more relevant concept is named support relation [15]–[17]. In support relation detection, it is usually assumed that objects could be properly represented by simple primitives, which restricts the application of such methods in the real world. Moreover, their performance will be affected by the upstream tasks (e.g. segmentation, geometry, and pose extraction, etc.). By contrast, it is believed that with large-scale datasets, integrating deep learning into traditional robotic techniques may bring improvements to the generality of the existing methods.

**Robotic grasping** has been an actively investigated area in robotics for a long time [18], but it still remains unsolved. Recently, with deep learning, researchers have achieved vast progress in robotic grasping (e.g. [1], [2], [7], [19]–[22]). Such methods heavily rely on large-scale grasp datasets such as Cornell Grasp Dataset<sup>2</sup>, DexNet [2], CMU Grasp Dataset [23], Jacquard Dataset [8], VMRD [5], and GraspNet [9]. Particularly, object-specific robotic grasping in clutter is a practical but harder problem, which recently attracts researchers devoted to it [5], [24], [25]. For example, [24] tries to detect grasps as well as the manipulation relationships with the model trained on VMRD [4]. However, it suffers from poor generality because of the limited dataset, which

severely restricts its practicality.

In this paper, we aim to build a new, large-scale, and automatically-generated grasp dataset considering all the above issues. We want to enable the robot to comprehensively percept the surroundings for grasp decision making.

## III. MODELING

We include multi-modal labels of the objects both in point clouds and RGB images. For object detection and segmentation, we follow the traditional settings in previous works [26]. The representation of object grasps and relationships will be introduced in detail in the following sections.

### A. Visual Manipulation Relationships

Following [4], REGRAD focuses on the pair-wise manipulation relationships between objects. Specifically, the manipulation relationship between the object pair  $(o_i, o_j)$  is a two-bit relationship  $R = (R_{ij}, R_{ji})$ , with each bit denoting whether the relationship  $R_{ij}$  or  $R_{ji}$  exists or not. If  $R_{ij} = 1$ , the object  $o_i$  should be grasped after  $o_j$ . Therefore, there are totally 4 kinds of manipulation relationships in REGRAD, which are demonstrated in Figure 3a.

### B. Grasps on Point Clouds

We demonstrate in Figure 3b how to define a grasp on the point cloud. Typically, a grasp usually involves 4 key components: the grasp point, the orientation of the gripper, the approaching vector, and the grasp quality. Therefore, a grasp on the point cloud can be formulated in Equation 1.

$$g_{pc} = (x, y, z, r_x, r_y, r_z, \theta, s) \quad (1)$$

where  $p_g = (x, y, z)$  defines the grasp point,  $\mathbf{r} = (r_x, r_y, r_z)$  defines the orientation of the gripper,  $\theta$  represents the approaching direction given  $p_g$  and  $\mathbf{r}$ , and  $s$  is a score of quality based on the antipodal measurement [22].

### C. Grasps on RGB Images

Typically, the 2D grasps are parameterized by oriented rectangles following the same settings from [27]:

$$g_{rect} = (x, y, w, h, \alpha) \quad (2)$$

with  $(x, y)$  representing the center of the grasp rectangle,  $(w, h)$  denoting the width and height, and  $\alpha$  being the

<sup>2</sup>[http://pr.cs.cornell.edu/grasping/rect\\_data/data.php](http://pr.cs.cornell.edu/grasping/rect_data/data.php)



counterclockwise orientation w.r.t. the horizontal axis of the image. Concretely, the  $(x, y)$  corresponds to the grasp point, and  $(w, h)$  defines the gripper shape with  $w$  being the distance between two fingers and  $h$  being the width of each finger. An example is given in Figure 3c.

#### IV. DATASET GENERATION

##### A. Preparation

1) *Object Models*: REGRAD is built on the basis of ShapeNet [10]. We split the categories into *seen* and *unseen* parts. The unseen categories will be used to generate data for validating and testing the performance of the trained models on completely unknown objects.

2) *Simulator*: In this paper, we use SAPIEN [28] as the simulator since it performs optimally compared with some other choices like PyBullet [29] and Gazebo [30] considering the trade-off among the speed, authenticity, and robustness.

##### B. Scene Generation

All the scenes are generated automatically in the same procedure. In general, we first randomly sample a number of objects from all the object models. After that, we load them one by one into the simulator, resulting in a random clutter scene.

1) *Object Randomization*: To load a model into the simulator, we need to define some parameters such as scale and friction. Specifically, to make the object graspable, we first sample a scale according to the longest side of the object's bounding box so that it is finalized in the range between 8cm and 20cm. For the friction, we sample the linear and angular damping coefficient between 1 and 1.5.

2) *Scene Randomization*: To generate a scene, we need to define the scene background and some necessary parameters. For the background, we use a random image to augment our dataset against the background noise for realistic tasks. For the light, we randomly import 1-4 light sources around the table, enabling rich light conditions. To load an object, we firstly sample an initial position above the table. Then the object will drop down freely from the initial position. To avoid severe collisions caused by high speed, we set the gravity acceleration of the simulator to 1/10 of the standard. After loading all objects, we will record all scene parameters and object states so that we can completely recover it later. For each scene, we will record the point clouds and RGB-D images from 9 different views as shown in Figure 4.

##### C. Manipulation Relationship Graph Generation

In this section, we will introduce the method to automatically label the manipulation relationship graph (MRG) for a given clutter scene. The manipulation relationship indicates the correct grasping order and the formal definition could be found in Section III-A. Some examples of MRG are given in the right column of Figure 2.

The main idea to generate MRG is that we can separately find out all the parent nodes of each node based on physical simulation. The procedure is summarized in Algorithm 1. Concretely, first of all, we initialize the scene using the

---

#### Algorithm 1 Algorithm of Automatically Generating MRG

---

**Require:** The set of objects  $O = \{o_i\}_{i=1}^{N_o}$ ; The object states  $S = \{s_{o_i}\}_{i=1}^{N_o}$ ; A pose error threshold  $\epsilon$ ;

- 1: Initialize the scene with the configuration recorded.
- 2: **for**  $i = 1, \dots, N_o$  **do**
- 3:   Initialize the parent list of node  $i$ :  $Par_i = \emptyset$
- 4:   **for**  $j = 1, \dots, N_o$  and  $j \neq i$  **do**
- 5:     Load  $o_j$  using state  $s_{o_j}$  in static mode.
- 6:     Load  $o_i$  using state  $s_{o_i}$  in non-static mode.
- 7:     **for**  $j = 1, \dots, N_o$  and  $j \neq i$  **do**
- 8:       Delete  $o_j$
- 9:       Run several simulation steps.
- 10:       Record  $o_i$ 's state  $s'_{o_i}$
- 11:       **if**  $|s'_{o_i} - s_{o_i}| > \epsilon$  **then**  $Par_i = Par_i \cup \{o_j\}$
- Recover  $o_i$  and  $o_j$ .
- return**  $MRG = \{Par_i\}_{i=1}^{N_o}$ ;

---

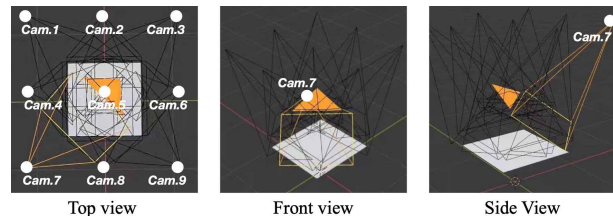


Fig. 4: Three views of the 9 different camera poses. All 9 positions are at the same height above the table, and located at the 9 intersections of the  $2 \times 2$  square grids.

recorded configuration without any objects (line 1). To find out the parent nodes of  $o_i$ , we firstly load  $o_i$  in non-static mode while all the other objects in static mode (line 4-6). The static mode means that the object cannot be affected by the simulation steps. Therefore, moving the ancestor but not parent nodes of  $o_i$  should not have a direct impact on  $o_i$ . Only the moving of parents will affect the balance of  $o_i$ . Thus, by iteratively moving all the other nodes, we can get a list of  $o_i$ 's parents (line 7-11). Finally, the parent lists of all nodes will result in a complete MRG for the given scene.

##### D. Grasp Generation

Basically, we follow the method introduced in [22] to generate 3D grasps and then follow [31] to project them onto RGB images to get 2D rectangular grasps.

1) *3D Grasps*: For grasp generation, we follow the flow of sample-first-then-filter. To be specific, we firstly sample a set of grasp candidates around each object by the following steps:

- **Point sampling** which samples a subset of points belonging to the object;
- **Depth sampling** which samples grasps with different depths along the direction of the surface normal at each point;
- **Rotation angle sampling** which samples different rotation angles around the surface normal at each point;

- **Inclination angle sampling** which samples different inclination angles around the vector between two fingers, namely different  $\theta$ s as shown in Figure 3b.

The sampled grasp pose of the gripper determines the approaching vector, which is within the gripper plane and perpendicular to the vector between two fingers, as well as the contact points when executing the grasping actions. After that, we conduct the static collision checking, which means that we only consider the final pose of the gripper without movement, and filter out all grasps with collisions. Finally, we assign an analytically-computed antipodal score and a center score to measure the quality of each grasp.

To get the *antipodal score*  $c_a$ , we follow S<sup>4</sup>G [22]. Besides, we assume that the high-quality grasps are usually located near the center of mass. Given the assumption of uniform mass distribution, the mass center usually coincides with the geometric center. Therefore, we assign the *center score*  $c_c$  describing the distance from the grasp to the geometric center of the object:

$$c_c = \frac{d_{max} - d}{d_{max} - d_{min}}$$

where  $d$  is the distance from the grasp to the object center,  $d_{max}$  and  $d_{min}$  are the maximum and minimum distance between any grasp and its corresponding object center.

2) *2D Grasps*: Our 2D rectangular grasps on RGB images are generated automatically using the projection of the 3D grasps from the point clouds.

To generate the 2D grasps on RGB images, first and foremost, we assume that the extrinsic and intrinsic parameters of the camera are available, which always holds in the simulator. Given a grasp representation from point clouds, we can easily obtain the grasp pose of the gripper. Provided the gripper pose, we define the two surfaces of the two fingers facing inward as the contact surface. Then we record the two edges at the bottom of the two contact surfaces and project them to the image frame through the camera parameters, resulting in a grasp parallelogram. The final grasp rectangle is defined as the minimum bounding rectangle of the grasp parallelogram. Finally, to discard inferior grasps, we filter out the grasp rectangles projected from the 3D grasp poses that have an angle larger than  $30^\circ$  with the camera.

## V. EXPERIMENTS

To validate the effectiveness of REGRAD, we run experiments on manipulation relationship detection and grasp detection on it. Results show that models trained on REGRAD could generalize well to realistic scenarios.

### A. Manipulation Relationship Detection

We firstly compare the performance of manipulation relationship detection on REGRAD and VMRD. The difference between these two datasets in terms of manipulation relationships is shown in Table III. To conduct the experiments, we test the performance on three validation datasets with comparison to VMRD [4]:

- **REGRAD-seen-val-500**: the first 500 scenes of REGRAD unseen-val set, consisting of 4500 images including different object instances of known categories.
- **REGRAD-unseen-val-500**: the first 500 scenes of REGRAD unseen-val set, consisting of 4500 images of unknown objects.
- **Sim-to-real transfer**: 200 realistic scenarios collected and labeled with real objects and a Kinect DK camera.

To do so, we implement the Visual Manipulation Relationship Network [4] on REGRAD, and train the model using the same settings. To make our model compatible with VMRD, we ignore the bidirectional relationship in REGRAD.

Note that to facilitate the sim-to-real transfer, we apply domain randomization techniques, i.e., a series of data augmentations are applied to the input images before we send them into the neural network. We conduct experiments using both RGB and depth images as the inputs. For RGB images, the standard augmentation, which is the same as the one in [4], is performed before the image is input to the neural network. While for depth images, we impose the augmentation to make the augmented images similar to the real ones. In detail, our augmentation includes:

- Random Gaussian noise with standard derivation from 0 to 2.5.
- Random granularity of 2.5 pixels to 5 pixels.
- Random Gaussian blurring with different kernel sizes.
- Random black holes on the edge of each object implemented using image high-pass filter.
- Random strip noise by adding a gray strip image onto the original image.
- Random brightness by multiplying the depth image with a random factor ranging from 0.6 to 1.2.

The first three augmentations will be executed with a random number of iterations for each depth image.

The evaluation metrics include recall, precision, and image accuracy as in [4]. However, since we are willing to compare the relationship performance on unknown objects, here we ignore the object detection part and use the ground truth bounding box for pure relationship classification. We respectively evaluate the performance of different kinds of relationships including parent relation (**P**), child relation (**C**), and no relation (**N**), and the results are shown in Table II. We can conclude that:

- The model trained on RGB images has a higher recall. This is because the RGB-based model is more aggressive, tending to misclassify the object pair with no relation to parent or child relation.
- The model trained on depth images has a much higher precision and image accuracy on all three validation sets. Also, it transfers better to the real scenarios, with nearly no performance loss and much higher precision, while the model trained on RGB images suffers from a severe sim-to-real performance loss.
- The prediction of no relation is more reliable than the one of parent and child relation due to data imbalance.
- The model trained on VMRD cannot generalize well to

TABLE II: Manipulation Relationship Detection

Metrics	Training Data	Performance											
		REGRAD-seen-val-500				REGRAD-unseen-val-500				Sim-to-real Transfer			
		P	C	N	Mean	P	C	N	Mean	P	C	N	Mean
Recall	VMRD-4683	17.59	22.55	95.78	45.31	16.48	21.35	95.46	44.43	22.82	26.97	97.02	48.94
	REGRAD5K-RGB	<b>60.88</b>	<b>60.87</b>	95.82	<b>72.52</b>	<b>55.24</b>	<b>54.32</b>	95.00	<b>68.19</b>	<b>90.04</b>	<b>73.03</b>	92.34	<b>85.14</b>
	REGRAD5K-Depth	59.11	55.90	<b>97.62</b>	70.88	52.27	48.58	<b>96.93</b>	65.93	77.18	61.83	<b>97.99</b>	79.00
Precision	VMRD-4683	21.27	19.86	95.67	45.60	21.44	19.57	95.00	45.34	25.94	22.49	97.17	48.53
	REGRAD5K-RGB	44.22	43.30	<b>98.12</b>	61.88	39.82	39.46	<b>97.58</b>	58.95	29.05	27.16	<b>99.74</b>	51.98
	REGRAD5K-Depth	<b>54.76</b>	<b>57.56</b>	97.77	<b>70.03</b>	<b>48.71</b>	<b>50.11</b>	97.07	<b>65.30</b>	<b>50.00</b>	<b>57.53</b>	99.19	<b>68.91</b>
Image Acc	VMRD-4683			13.4				15.5				16.1	
	REGRAD5K-RGB			22.2				19.6				17.6	
	REGRAD5K-Depth			<b>27.4</b>				<b>24.5</b>				<b>40.7</b>	

TABLE III: Comparison with VMRD

	VMRD [4]	REGRAD	Times
None	24.9K	<b>11.38M</b>	~ <b>455</b>
Parent	13.3K	<b>430.7K</b>	~ <b>33</b>
Child	13.3K	<b>430.7K</b>	~ <b>33</b>
Bidirectional	-	<b>81.6K</b>	-
Total	51.5K	<b>12.32M</b>	~ <b>240</b>

TABLE IV: Comparison with REGNet Dataset

	MAS	MNG	MNG(0.5)
REGNet [3]	0.5623	294	196
REGRAG	0.5000	1040	503

new object instances, showing the worst generalization performance.

### B. Grasp Detection

We test the 3D grasp detection performance on REGRAD based on the state-of-the-art grasp detector REGNet [3] following the same settings. To evaluate whether the model trained on REGRAD can generalize well, we also conduct the cross-dataset validation by deploying two models on REGRAD and REGNet datasets [3]. Following [3], we use two metrics to evaluate the grasp performance: collision-free ratio and antipodal score, which describe the possibility of each grasp having no collision with objects and the force-closure property respectively.

Table IV shows the differences between REGRAD and REGNet datasets. *MAS* denotes the mean antipodal score, *MNG* represents the mean number of grasps, and *MNG(0.5)* is *MNG* with an antipodal score larger than 0.5. The results are illustrated in Table V, where *Cf-R* is the average collision-free rate and *AS* is the average antipodal score provided the detected grasps. We can conclude that:

- REGRAD has denser labels in each scene than REGNet dataset.
- The model trained on REGRAD generalizes well to REGNet dataset, with low collision rate and high antipodal score.
- The model trained on REGNet only works well on REGNet dataset and suffers from a sharp drop of

TABLE V: Cross-dataset Grasp Detection Performance

Train	Test	Cf-R	AS
REGNet [3]	REGNet [3]	82.11%	0.5690
REGNet [3]	REGRAD	78.53%	0.3741
REGRAD	REGNet [3]	81.32%	0.5651
REGRAD	REGRAD	79.32%	0.4353

TABLE VI: Real-robot Grasping Performance

Training Data	Success Rate	Complete Rate
REGNet [3]	79.34%	96.00%
REGRAD	86.63%	96.17%

performance when transferred to REGRAD.

- REGRAD is harder than REGNet dataset. Both models perform worse on REGRAD compared to REGNet dataset, since 1) the large number of non-convex models in REGRAD leads to a lower antipodal score, and 2) the scenarios in REGRAD are more complicated.

We also conducted the real-robot experiments to execute the detected grasps in real-world scenarios, and the results are shown in Table VI. In detail, we run the models in 10 different scenarios, including 6-12 objects which are stacked together. The grasping procedure will end until there is no available grasp detected anymore. We can see that benefitting from the large-scale dataset, the model trained on REGRAD has a higher grasp success rate (86.63%) compared to the model trained on REGNet dataset (79.34%) in the real world.

## VI. CONCLUSIONS AND FUTURE WORK

In this paper, we contribute a large-scale and automatically-generated relational grasping dataset, namely REGRAD (Relational GRASP Dataset). Our dataset is the first one targeting comprehensive perceptual tasks in robotic manipulation, including object and pose detection, segmentation, target-driven grasping, and relationship understanding. Along with the dataset, we also provide a principled way to automatically generate relation labels for deep-learning-based manipulation, meeting the data-intensive models. We also implemented a series of

state-of-the-art algorithms on REGRAD, serving as the baselines.

For future work, we aim to expand REGRAD using object captions for human-robot interaction. The model-wise captions from ShapeGlot [32] can be used for generating image-wise dense captions automatically by leveraging the spatial relationships and the relative positions among objects. We also intend to expand REGRAD with more sophisticated relationships. Notably, the current definition of manipulation relationship is simple, object-agnostic, yet sufficient for most cases. However, in our practice, the manipulation relationships among objects are subtle. The relationship should sometimes depend on the attributes of the objects, e.g., the mass distribution and fragility. For example, when a pen (instead of a cup) is on top of a book, we tend to grasp the book directly since this grasping action is harmless. Therefore, taking into consideration of object attributes in the MRG is promising to improve the efficiency of the current algorithm. Also, the relationships could depend on the action itself [33], [34]. In our current formulation, the manipulation relationship is only considered in the context of grasping. However, by formulating the tuple of object-action-object, the MRG could support more flexible manipulations.

Finally, there will be a wide range of possible directions based on REGRAD, for example:

1) *Object-Agnostic Manipulation Relationship Detection*: As mentioned, despite its simplicity and suboptimality, the current object-agnostic definition of manipulation relationship is sufficient for most cases. Yet, its robust detection still remains unsolved, especially for unknown objects. Some visual relationship detection algorithms raise up interesting perspectives for object-agnostic relationship detection [35]–[37]. Such ideas (e.g. introducing network structure bias to alleviate the object-specific features and adversarial training) are hopeful to be further explored to detect manipulation relations between unknown objects. Besides, support relation analysis could generalize well to unknown objects [15]–[17], [38], [39] provided the physical properties like mass distribution and friction coefficient [16] or assumptions that objects could be properly approximated by simple geometric primitives [15], [17], [38], [39]. To follow such ideas in the future, the main challenge is how to get rid of the strong reliance on physical properties and geometric assumptions.

2) *Target-driven Grasp Detection in Clutter*: Target-driven grasping should be based on robust object-specific grasp detection. To achieve so, one possible way is utilizing object-specific features to detect grasps in point clouds. Fortunately, recent advances in deep learning show promising ways for extracting point cloud features (e.g. [40]–[43]). Based on the advanced point cloud feature extractor, we will try to solve the following problems of target-driven grasping in dense clutter in the future:

- Develop object-specific grasping feature extractors.
- Segment unknown objects accurately in clutter.
- Design robust object-specific grasp detector.
- Filter out grasps that are not for the targets.
- Avoid potential collisions when grasping.

3) *Sim-to-Real Transfer Learning*: Since REGRAD is generated automatically using the physical simulator, there exists a reality gap between the training data and realistic scenarios. Therefore, facing the challenges of sim-to-real is a practical and important issue. Currently, there are mainly three ways toward solving this problem: *fine-tune*, *domain randomization* [44], and *domain adaptation* [45]. Fine-tune means training on simulative data while followed by a fine-tune stage using real-world data, which would dramatically reduce the data amount required by training from scratch (e.g. [46], [47]). However, though the requirements are relaxed, it still needs a real-world dataset with a considerable size, which would be time-consuming to collect. Domain randomization usually defines a diversified data space in the simulator, in which the real-world data are assumed to be. By contrast, the key idea of domain adaptation is to build a shared space when given one or more *source* domains (e.g. the simulative data) and a *target* domain (the realistic data). In this paper, we have already verified the vanilla domain randomization techniques, which successfully help our models, especially the depth-based model, transfer to real-world scenarios. In the future, we could also consider the domain adaptation method based on adversarial learning [48], [49] and contrastive learning [50], [51] to improve the sim-to-real performance.

We believe that REGRAD will provide robotics researchers with more chances to face the challenges of complex robotic manipulation tasks.

## REFERENCES

- [1] J. Redmon and A. Angelova, “Real-time grasp detection using convolutional neural networks,” in *2015 IEEE International Conference on Robotics and Automation (ICRA)*. IEEE, 2015, pp. 1316–1322.
- [2] J. Mahler, F. T. Pokorny, B. Hou, M. Roderick, M. Laskey, M. Aubry, K. Kohlhoff, T. Kröger, J. Kuffner, and K. Goldberg, “Dex-net 1.0: A cloud-based network of 3d objects for robust grasp planning using a multi-armed bandit model with correlated rewards,” in *2016 IEEE international conference on robotics and automation (ICRA)*. IEEE, 2016, pp. 1957–1964.
- [3] B. Zhao, H. Zhang, X. Lan, H. Wang, Z. Tian, and N. Zheng, “Regnet: Region-based grasp network for single-shot grasp detection in point clouds,” *arXiv preprint arXiv:2002.12647*, 2020.
- [4] H. Zhang, X. Lan, X. Zhou, Z. Tian, Y. Zhang, and N. Zheng, “Visual manipulation relationship network for autonomous robotics,” in *2018 IEEE-RAS 18th International Conference on Humanoid Robots (Humanoids)*. IEEE, 2018, pp. 118–125.
- [5] H. Zhang, X. Lan, S. Bai, X. Zhou, Z. Tian, and N. Zheng, “RoI-based robotic grasp detection for object overlapping scenes,” in *2019 IEEE/RSJ International Conference on Intelligent Robots and Systems (IROS)*. IEEE, 2019, pp. 4768–4775.
- [6] Y. LeCun, Y. Bengio, and G. Hinton, “Deep learning,” *nature*, vol. 521, no. 7553, pp. 436–444, 2015.
- [7] S. Levine, P. Pastor, A. Krizhevsky, J. Ibarz, and D. Quillen, “Learning hand-eye coordination for robotic grasping with deep learning and large-scale data collection,” *The International Journal of Robotics Research*, vol. 37, no. 4-5, pp. 421–436, 2018.
- [8] A. Depierre, E. Dellandréa, and L. Chen, “Jacquard: A large scale dataset for robotic grasp detection,” in *2018 IEEE/RSJ International Conference on Intelligent Robots and Systems (IROS)*. IEEE, 2018, pp. 3511–3516.
- [9] H.-S. Fang, C. Wang, M. Gou, and C. Lu, “Graspnet-1billion: A large-scale benchmark for general object grasping,” in *Proceedings of the IEEE/CVF Conference on Computer Vision and Pattern Recognition*, 2020, pp. 11 444–11 453.

- [10] Z. Wu, S. Song, A. Khosla, F. Yu, L. Zhang, X. Tang, and J. Xiao, "3d shapenets: A deep representation for volumetric shapes," in *Proceedings of the IEEE conference on computer vision and pattern recognition*, 2015, pp. 1912–1920.
- [11] A. X. Chang, T. Funkhouser, L. Guibas, P. Hanrahan, Q. Huang, Z. Li, S. Savarese, M. Savva, S. Song, H. Su *et al.*, "Shapenet: An information-rich 3d model repository," *arXiv preprint arXiv:1512.03012*, 2015.
- [12] C. Lu, R. Krishna, M. Bernstein, and L. Fei-Fei, "Visual relationship detection with language priors," in *European conference on computer vision*. Springer, 2016, pp. 852–869.
- [13] R. Krishna, Y. Zhu, O. Groth, J. Johnson, K. Hata, J. Kravitz, S. Chen, Y. Kalantidis, L.-J. Li, D. A. Shamma *et al.*, "Visual genome: Connecting language and vision using crowdsourced dense image annotations," *International journal of computer vision*, vol. 123, no. 1, pp. 32–73, 2017.
- [14] B. Rosman and S. Ramamoorthy, "Learning spatial relationships between objects," *The International Journal of Robotics Research*, vol. 30, no. 11, pp. 1328–1342, 2011.
- [15] S. Panda, A. A. Hafez, and C. Jawahar, "Learning support order for manipulation in clutter," in *2013 IEEE/RSJ International Conference on Intelligent Robots and Systems*. IEEE, 2013, pp. 809–815.
- [16] R. Mojtahedzadeh, A. Bouguerra, E. Schaffernicht, and A. J. Lilienthal, "Support relation analysis and decision making for safe robotic manipulation tasks," *Robotics and Autonomous Systems*, vol. 71, pp. 99–117, 2015.
- [17] R. Kartmann, F. Paus, M. Grotz, and T. Asfour, "Extraction of physically plausible support relations to predict and validate manipulation action effects," *IEEE Robotics and Automation Letters*, vol. 3, no. 4, pp. 3991–3998, 2018.
- [18] J. Bohg, A. Morales, T. Asfour, and D. Kragic, "Data-driven grasp synthesis—a survey," *IEEE Transactions on Robotics*, vol. 30, no. 2, pp. 289–309, 2013.
- [19] I. Lenz, H. Lee, and A. Saxena, "Deep learning for detecting robotic grasps," *The International Journal of Robotics Research*, vol. 34, no. 4-5, pp. 705–724, 2015.
- [20] S. Kumra and C. Kanan, "Robotic grasp detection using deep convolutional neural networks," in *2017 IEEE/RSJ International Conference on Intelligent Robots and Systems (IROS)*. IEEE, 2017, pp. 769–776.
- [21] J. Mahler, M. Matl, V. Satish, M. Danielczuk, B. DeRose, S. McKinley, and K. Goldberg, "Learning ambidextrous robot grasping policies," *Science Robotics*, vol. 4, no. 26, 2019.
- [22] Y. Qin, R. Chen, H. Zhu, M. Song, J. Xu, and H. Su, "S4g: Amodal single-view single-shot se (3) grasp detection in cluttered scenes," in *Conference on robot learning*. PMLR, 2020, pp. 53–65.
- [23] L. Pinto and A. Gupta, "Supersizing self-supervision: Learning to grasp from 50k tries and 700 robot hours," in *2016 IEEE international conference on robotics and automation (ICRA)*. IEEE, 2016, pp. 3406–3413.
- [24] H. Zhang, X. Lan, S. Bai, L. Wan, C. Yang, and N. Zheng, "A multi-task convolutional neural network for autonomous robotic grasping in object stacking scenes," in *2019 IEEE/RSJ International Conference on Intelligent Robots and Systems (IROS)*. IEEE, 2019, pp. 6435–6442.
- [25] A. Murali, A. Mousavian, C. Eppner, C. Paxton, and D. Fox, "6-dof grasping for target-driven object manipulation in clutter," in *2020 IEEE International Conference on Robotics and Automation (ICRA)*. IEEE, 2020, pp. 6232–6238.
- [26] T.-Y. Lin, M. Maire, S. Belongie, J. Hays, P. Perona, D. Ramanan, P. Dollár, and C. L. Zitnick, "Microsoft coco: Common objects in context," in *European conference on computer vision*. Springer, 2014, pp. 740–755.
- [27] Y. Jiang, S. Moseson, and A. Saxena, "Efficient grasping from rgb-d images: Learning using a new rectangle representation," in *2011 IEEE International conference on robotics and automation*. IEEE, 2011, pp. 3304–3311.
- [28] F. Xiang, Y. Qin, K. Mo, Y. Xia, H. Zhu, F. Liu, M. Liu, H. Jiang, Y. Yuan, H. Wang *et al.*, "Sapien: A simulated part-based interactive environment," in *Proceedings of the IEEE/CVF Conference on Computer Vision and Pattern Recognition*, 2020, pp. 11 097–11 107.
- [29] E. Coumans and Y. Bai, "Pybullet, a python module for physics simulation for games, robotics and machine learning," 2016.
- [30] N. Koenig and A. Howard, "Design and use paradigms for gazebo, an open-source multi-robot simulator," in *2004 IEEE/RSJ International Conference on Intelligent Robots and Systems (IROS)(IEEE Cat. No. 04CH37566)*, vol. 3. IEEE, 2004, pp. 2149–2154.
- [31] C. Yang, X. Lan, H. Zhang, and N. Zheng, "Task-oriented grasping in object stacking scenes with crf-based semantic model," in *2019 IEEE/RSJ International Conference on Intelligent Robots and Systems (IROS)*. IEEE, 2019, pp. 6427–6434.
- [32] P. Achlioptas, J. Fan, R. Hawkins, N. Goodman, and L. J. Guibas, "Shapeglot: Learning language for shape differentiation," in *Proceedings of the IEEE/CVF International Conference on Computer Vision*, 2019, pp. 8938–8947.
- [33] Y. Sun, S. Ren, and Y. Lin, "Object-object interaction affordance learning," *Robotics and Autonomous Systems*, vol. 62, no. 4, pp. 487–496, 2014.
- [34] K. Mo, Y. Qin, F. Xiang, H. Su, and L. Guibas, "O2o-afford: Annotation-free large-scale object-object affordance learning," *arXiv preprint arXiv:2106.15087*, 2021.
- [35] H. Zhang, Z. Kyaw, S.-F. Chang, and T.-S. Chua, "Visual translation embedding network for visual relation detection," in *Proceedings of the IEEE conference on computer vision and pattern recognition*, 2017, pp. 5532–5540.
- [36] X. Yang, H. Zhang, and J. Cai, "Shuffle-then-assemble: Learning object-agnostic visual relationship features," in *Proceedings of the European conference on computer vision (ECCV)*, 2018, pp. 36–52.
- [37] Z.-S. Hung, A. Mallya, and S. Lazebnik, "Contextual translation embedding for visual relationship detection and scene graph generation," *IEEE transactions on pattern analysis and machine intelligence*, 2020.
- [38] M. Grotz, D. Sippel, and T. Asfour, "Active vision for extraction of physically plausible support relations," in *2019 IEEE-RAS 19th International Conference on Humanoid Robots (Humanoids)*. IEEE, 2019, pp. 439–445.
- [39] F. Paus and T. Asfour, "Probabilistic representation of objects and their support relations," in *International Symposium on Experimental Robotics*, 2021, pp. 510–519.
- [40] C. R. Qi, H. Su, K. Mo, and L. J. Guibas, "Pointnet: Deep learning on point sets for 3d classification and segmentation," in *Proceedings of the IEEE conference on computer vision and pattern recognition*, 2017, pp. 652–660.
- [41] P. Ni, W. Zhang, X. Zhu, and Q. Cao, "Pointnet++ grasping: Learning an end-to-end spatial grasp generation algorithm from sparse point clouds," *arXiv preprint arXiv:2003.09644*, 2020.
- [42] M.-H. Guo, J.-X. Cai, Z.-N. Liu, T.-J. Mu, R. R. Martin, and S.-M. Hu, "Pct: Point cloud transformer," *arXiv preprint arXiv:2012.09688*, 2020.
- [43] J. Wang, R. Chakraborty, and X. Y. Stella, "Spatial transformer for 3d point clouds," *IEEE Transactions on Pattern Analysis and Machine Intelligence*, 2021.
- [44] J. Tobin, R. Fong, A. Ray, J. Schneider, W. Zaremba, and P. Abbeel, "Domain randomization for transferring deep neural networks from simulation to the real world," in *2017 IEEE/RSJ international conference on intelligent robots and systems (IROS)*. IEEE, 2017, pp. 23–30.
- [45] M. Wang and W. Deng, "Deep visual domain adaptation: A survey," *Neurocomputing*, vol. 312, pp. 135–153, 2018.
- [46] A. A. Rusu, M. Večerík, T. Rothörl, N. Heess, R. Pascanu, and R. Hadsell, "Sim-to-real robot learning from pixels with progressive nets," in *Conference on Robot Learning*. PMLR, 2017, pp. 262–270.
- [47] Y. Chebotar, A. Handa, V. Makovychuk, M. Macklin, J. Issac, N. Ratliff, and D. Fox, "Closing the sim-to-real loop: Adapting simulation randomization with real world experience," in *2019 International Conference on Robotics and Automation (ICRA)*. IEEE, 2019, pp. 8973–8979.
- [48] S. Wang, X. Chen, Y. Wang, M. Long, and J. Wang, "Progressive adversarial networks for fine-grained domain adaptation," in *Proceedings of the IEEE/CVF conference on computer vision and pattern recognition*, 2020, pp. 9213–9222.
- [49] M. Xu, J. Zhang, B. Ni, T. Li, C. Wang, Q. Tian, and W. Zhang, "Adversarial domain adaptation with domain mixup," in *Proceedings of the AAAI Conference on Artificial Intelligence*, vol. 34, no. 04, 2020, pp. 6502–6509.
- [50] W. Liu, D. Ferstl, S. Schuster, L. Zebedin, P. Fua, and C. Leistner, "Domain adaptation for semantic segmentation via patch-wise contrastive learning," *arXiv preprint arXiv:2104.11056*, 2021.
- [51] M. Thota and G. Leontidis, "Contrastive domain adaptation," *arXiv preprint arXiv:2103.15566*, 2021.